Research Square

Preprints are preliminary reports that have not undergone peer review.
They should not be considered conclusive, used to inform clinical practice,
or referenced by the media as validated information.

Investigation of Low Frequency Noise-current Correlation for the InAs/GaSb T2SL Long-wavelength Infrared Detector

Liang Wang (786936165@qq.com)
University of the Chinese Academy of Sciences https://orcid.org/0000-0002-7106-5093
Liqi Zhu
ShanghaiTech University
Zhicheng Xu
Shanghai Institute of Technical Physics
Fangfang Wang
Shanghai Institute of Technology
Jianxin Chen
Shanghai Institute of Technical Physics
Baile Chen
ShanghaiTech University

Research Article

Keywords: T2SL, long-wavelength, infrared detector, low frequency noise, 1/f noise

Posted Date: July 12th, 2021

DOI: https://doi.org/10.21203/rs.3.rs-487224/v1

License: This work is licensed under a Creative Commons Attribution 4.0 International License.
Read Full License

Investigation of low frequency noise-current correlation for the InAs/GaSb T2SL long-wavelength infrared detector

Wang liang[12]，Zhu liqi[123]，Xu zhicheng[2]，Wang fangfang[2]，Chen jianxin[2]，Chen baile[3]

[1]University of Chinese Academy of Sciences
[2]Shanghai Institute of Technical Physics, Chinese Academy of Sciences
[3]School of Information Science and Technology, Shanghai Tech University

Abstract

In this paper, a mesa-type 256×8 long-wavelength infrared detector is prepared by using InAs/GaSb type-II superlattice material with double barrieres structure. the area of each pixel is 25×25 μm^2. The cut-off wavelength and dark current density of the detector at -0.05 V bias with liquid nitrogen temperature is 11.5 μm and 4.1×10^{-4} A/cm^2, respectively. The power spectrum of low-frequency noise (*1/f* noise) at different temperatures have also been fitted by the Hooge model, and the correlations with dark current are extracted subsequently. The results shown that the *1/f* noise of the detector is mainly caused by the generation-recombination current at a low reverse bias, however, when the reverse bias is high, the *1/f* noise should be expressed by the sum of I_{gr} noise and I_{btb} noise which is ignored in the previous research. The *1/f* noise-current correlation assessed in this work can provide insights into the low frequency noise characteristics of long-wavelength T2SL InAs/GaSb detectors, and allow for a better understanding of the main source of low-frequency noise.

Key world: T2SL, long-wavelength, infrared detector, low frequency noise, *1/f* noise

Introduction

Since Smith and Mailhiot proposed the possibility of superlattice in the last century [1], because of the advantage of low auger recombination rate, low tunneling current, flexible band gap engineering, and high uniformity [2], InAs/GaSb type-II superlattice (T2SL) has been developed into an important material system for long-wavelength infrared detection. For a InAs/GaSb T2SL detector, electrical noise, as an important merit, is always used to define the signal-to-noise ratio and determine the “true” detectivity, which includes frequency-independent shot noise, thermal noise and frequency-dependent generate-recombination (g-r) noise, *1/f* noise.

In general, the *1/f* noise is considered as the major influence of device performance, although many studies have been done before [3-9], it still has no precise or general physical model to perform in infrared device noise analysis. Baile Chen et al. studied the origin of *1/f* noise in $Hg_{1-x}Cd_xTe$ detectors and founded that the *1/f* noise mainly comes from diffusion current (I_{diff}), generation-recombination current (I_{gr}), and shunt current (I_{shunt}) [10]. However, different from the way of MCT changing the material composition, T2SL engineers its effective band gap by adjusting the thickness of layers. Therefore, the mini energy band of T2SL is much more complex and the role of band-to-band tunneling current (I_{btb}) in the process of noise generation should not been ignored. For this

reason, we would like to understand whether the *1/f* noise is related to band-to-band tunneling current, so that we can improve the performance of InAs/GaSb detectors at low frequency.

In this paper, system work has been done to analysis the noise characteristic of InAs/GaSb T2SL long-wavelength infrared detector. we simulated the dark current dates at liquid nitrogen temperature with different biases to get the main parameters related to dark current firstly. Then we optimized these parameters through bias-dependence dark current fitting at variable temperatures. Finally, the noise coefficient of different dark currents at different experimental conditions are performed based on Hooge's model.

Device and Measurements

In this experiment, a double barrier structure was used. The specific details have been introduced in the previous article [11]. Compared with single barrier structure, the structure can reduce Shockley–Read–Hall processes in the depletion region, and restrain the movement of majority carriers to low the diffusion dark currents more effectively. [12]

The epitaxial material was grown biased on a 3-inch n-type GaSb (100) substrate by a solid source molecular beam epitaxy system. The format of the detector arrays is 256×8 and the area of each pixel is 25×25 μm^2. For further electrical characterization, the detector was mounted into a liquid-nitrogen-cooled Dewar, the spectral response was tested by a Fourier transform infrared spectrometer, the dark current of the detector was tested by 6430 Semiconductor Analyzer, and the low frequency noise of the detector was measured by FS-PRO Dynamic Signal Analyzer. As shown in Fig.1, the 100% cut-off wavelength of the device is about 11.5 μm, which indicates the E_g of the detector is about 0.109 eV at a liquid nitrogen temperature.

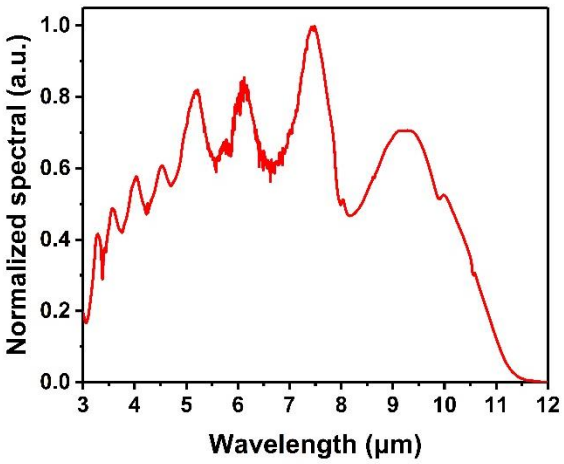

Fig.1 Normalized spectrum of the detector.

Results and discussion

At present, *1/f* noise is recognized to be sensitive to the material growth quality and the passivation process of device [13], which will introduce some surface states or impurity defects to a certain extent. However, there is no a universal model to forecast the exact *1/f* noise value for a given detector. In the *1/f* noise research, the most usual method which is also applied in this study is the Hooge model [14], by this model, the individual contribution of each dark current to the total *1/f* noise can be expressed as the following formula

$$S_i(f) = \sum_k \boldsymbol{\alpha}_k I_k^{\beta_k}/f \quad (1)$$

where $S_i(f)$ means the total *1/f* noise power special density (PSD), I_k is the k-component of the dark currents that have contribution to the total PSD. α_k and β_k are the noise coefficient and the current exponent of k-component, respectively.

I The simulation of dark current

Before studying the dependences of *1/f* noise and dark currents, different kinds of dark current should be decomposed firstly. Usually, the dark current of infrared photodetectors is composed of the following five components: band-to-band tunneling current, trap-assisted tunneling current (I_{tat}), generation-recombination current, diffusion current and surface leakage current [15]. It is worth mentioning that, in this report, there was no surface leakage current component was found through the fabrication of detectors with different perimeter-area-ratios (P/A), as shown in Fig.2.

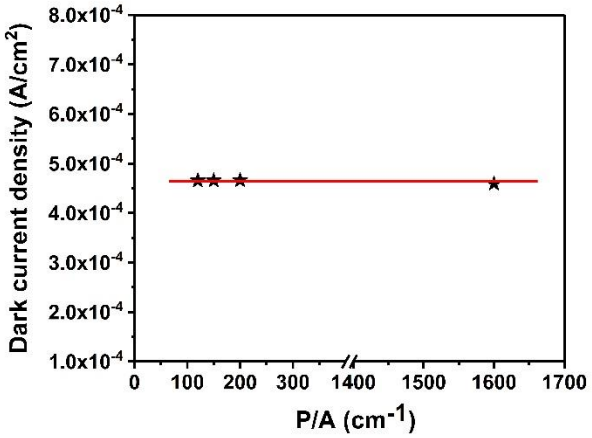

Fig.2 The dark current density of devices with different perimeter-area-ratios at 77 K, -0.05 V bias.

Based on the expression of each dark current component we can find that, I_{diff} has a liner relation with $e^{\frac{1}{kT}}$, I_{gr} is positively related to $e^{\frac{1}{2kT}}$ while I_{tat} and I_{btb} are temperature independent. Therefore, according to the relationship between the dark current of detector and the temperature, the activation energy of the detector can be calculated. Thereby, it is possible to analyze which kind of the dark current in the detector is the main mechanism in a specific temperature range.

As shown in Fig.3, the dark currents were obtained at the temperature of 40 K to 200 K with the bias voltage of -0.05 V and -0.5 V. For fig. 3(a) V=-0.05 V, it indicates an active energy about 0.0478 eV, about half of the bandgap energy, when the temperature below to 60 K. It also demonstrates that the main mechanism of the dark current is the generation-recombination current. As the temperature rises, the diffusion current component increases gradually and the detector becomes diffusion-limited from 140 K onward. But for fig. 3(b) V=-0.5 V, when the temperature is lower than 60 K, the active energy is close to 0 eV which demonstrates that the tunneling current is playing a key role of the dark current in this temperature range. However, when the temperature increases to 120 K, the diffusion current is coming to work with an active energy about 0.1073 eV. In conclusion, the diffusion current is the dominant current at high temperature whether it stands at low or high reverse bias.

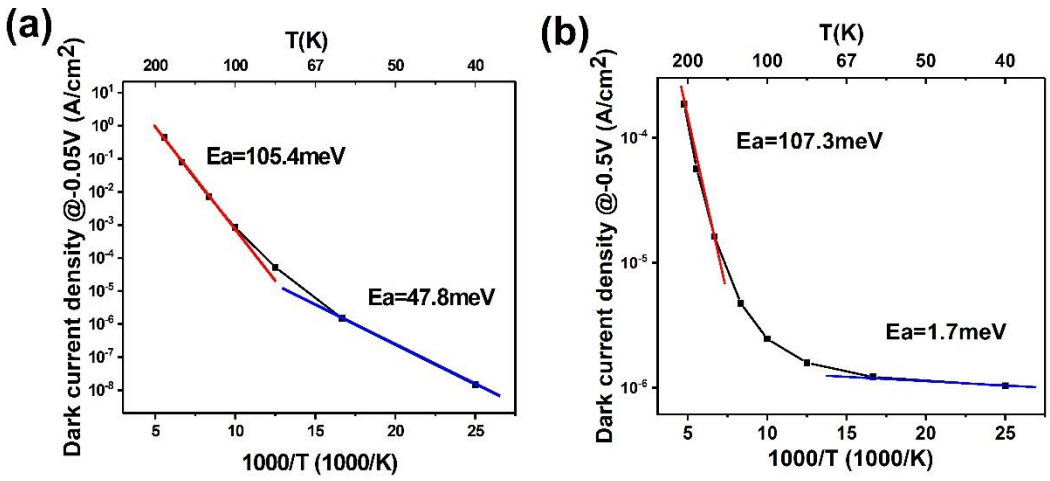

Fig.3 The relationship between temperature and dark current density, at different reverse biases of (a)-0.05 V and (b)-0.5 V.

In order to have an in-depth understanding of the influence of different dark currents on the overall current at different measure conditions, we simulated the dark currents at different temperatures using the expressions in the Ref.15 with the bias voltage between -0.01 V to -0.5 V. Fig.4 shows the experimental and simulated dark current with the conventional photodetector theory model at 80 K, it can be seen from the picture, the model established by us can fit the experimental data well. The values of partial parameters used are shown in table.1. The dark current density at 80 K and -0.05 V is only 4.1×10^{-4} A/cm^2 which is considerably lower and indicates an extremely high performance. When the reverse bias is -0.3~0 V, the dominant mechanism of dark current is I_{gr}, which is consistent with the previous fitting results of dark currents under variable temperature at -0.05 V. On the other hand, when the revise bias is higher than -0.3 V, I_{btb} comes to be the main dark current. The inset pictures express that the simulation of total dark currents corresponding well to the measured results at all temperatures, which lays a foundation for the following noise analysis.

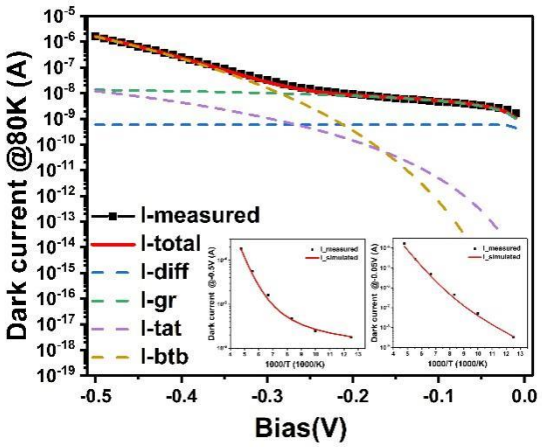

Fig. 4 Experimental and simulated dark current with the conventional photodetector theory model at 80 K, the inset is the temperature-dependence dark current fitting at -0.5 V and -0.05 V.

Table.1 values of partial parameters used in the simulation

parameters	values	units
doping concentration of acceptor N_A	2.2×10^{16}	cm^{-3}
doping concentration of donor N_D	1×10^{17}	cm^{-3}
effective mass of electronic m_e	0.019	M_0
effective mass of hole m_h	0.029	M_0
mobility of electronic μ_e	400*(T/45)^ (-1.5)	cm^2/Vs
mobility of hole μ_h	100	cm^2/Vs
effective band gap width E_g	(0.1087728-0.0002*(T-77))	ev
lifetime of electronic τ_e	200	ns
lifetime of hole τ_h	100	ns
lifetime of generation and recombination τ_{gr}	25	ns

II The noise power spectral density

Fig. 5 shows the noise PSD of the InAs/GaSb T2SL infrared detector at the reverse bias of -0.05 V and the temperature range of 80 K to 200 K. When the frequency is lower than 10^4 Hz, the noise shows a phenomenon that is inversely proportional to the frequency, called *1/f* noise. When the frequency increases to 10^4~10^6 Hz, the noise becomes almost frequency-independent, this is the result of white noise which generated by the random thermal motion of charge carriers [16]. It is also worth to know that as the temperature elevates, the value of the turning frequency is also rising due to the *1/f* noise covers the effects of white noise. There was no G-R noise was depicted in the spectral of noise power density curve which indicated the good quality of our material growth [17]. On the other hand, at 200 K temperature, the noise value at 1Hz is about 1×10^{17} A^2/Hz, which is relatively lower at high temperature.

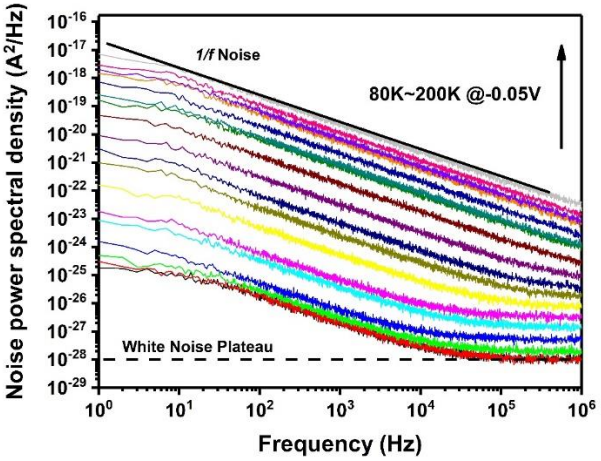

Fig. 5 the noise power spectral density of detector with variable temperature at -0.05 V

Fig.6 shows the measurements and fitting results of device's PSD at different temperatures and fixed revise bias (a) V= -0.05 V and (b) V= -0.5 V. The temperature range is 80 K to 200 K. Here the black point-lines present the measured data while the colorful lines are the fitting results. Previous study has shown that diffusion current has negligible impact on *1/f* noise [18], as the dominate dark current in low bias and high bias are I_{gr} and I_{btb}, respectively. Thus, the conventional

I_{gr} and I_{btb} are utilized to characterize the temperature dependence of noise PSD, the current exponents, β_{gr} and β_{btb}, are set to 2 and 1, respectively.

The simulation results show that, at low reverse bias of V=-0.05 V, *1/f* noise is generated entirely from generation and recombination currents in all temperature ranges. But for high reverse bias of V=-0.5 V, when the temperature is lower than about 120 K, band-to-band tunneling current is the main noise contributor with the α_{btb} of 3.4×10^{-14}. As the temperature rises, the noise related to generation and recombination current becomes more and more important and plays a leading role when temperature is higher than 150 K. It worth to know, the values of α_{gr} for the high and low revise biases are different, they are 7×10^{-8} and 2×10^{-8}, respectively.

Consequently, the total *1/f* noise for device at low reverse bias V=-0.05 V with temperature *T* and frequency *f* can be expressed by the sum of I_{gr} noise:

$$S_I(T,f) = \alpha_{gr} I_{gr}^2 / f \tag{2}$$

On the other hand, the total *1/f* noise for device at high reverse bias V=-0.5 V should be expressed by the sum of I_{gr} noise and I_{btb} noise

$$S_I(T,f) = [\alpha_{btb} I_{btb} + \alpha_{gr} I_{gr}^2]/f \tag{3}$$

Equations (2) and (3) conclude the relationship between dark current and *1/f* noise in InAs/GaSb T2SL detectors at different reverse biases with various operation temperature, which would provide a useful guidance to improve the performance of InAs/GaSb T2SL device especially for the 1/*f* noise reducing.

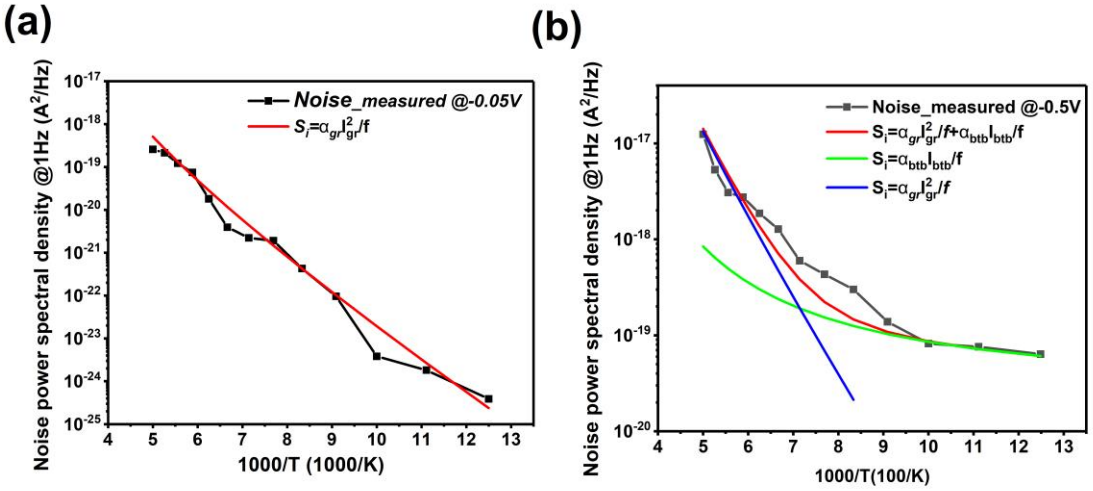

Fig.6 The measurements and fitting of PSD at different temperatures with reverse bias of (a)-0.05V and (b)-0.5V

Conclusion

In this work, the low frequency noise and dark current with various temperature and bias of InAs/GaSb T2SL infrared detector has been studied. There was no G-R noise was funded in our research which indicated the good growth quality of our material. It was also indicated that when revise bias is low, the total *1/f* noise for device can be expressed by I_{gr} noise. However, when the revise bias is large, the total *1/f* noise is indeed related to I_{btb} and can be expressed by the sum of I_{gr} noise and I_{btb} noise. The findings in this study may guide us to reduce the device noise and improve the signal-to-noise ratio of the detector.

References

[1] D. L. Smith, C. Mailhiot.: Proposal for strained type II superlattice infrared detectors. Journal of Applied Physics. 62(6), 2545-2548 (1987)

[2] H. Mohseni, V. I. Litvinov, M. Razeghi.: Interface-induced suppression of the Auger recombination in type-II InAs/GaSb superlattices. Physical Review B. 58(23), 15378–15380 (1998)

[3] S. H. Bae, S. J. Lee, Y. H. Kim, H. C. Lee, C. K. Kim.: Analysis of 1/f Noise in LWIR HgCdTe Photodiodes. Journal of Electronic Material. 29(6), 877-882 (2000)

[4] R. J. Westerhout, C.A. Musca, J. Antoszewski, J. M. Dell, L. Faraone.: Investigation of 1/f Noise Mechanisms in Midwave Infrared HgCdTe Gated Photodiodes. Journal of Electronic Material. 36(8), 884-889 (2007)

[5] L. H. Wan, X. M. Shao, Y. J. Ma, S. Y. Deng, Y. G. Liu, J. F. Cheng, Y. G, T. Li, X. Li.: Dark current and 1/f noise characteristics of $In_{0.74}Ga_{0.26}As$ photodiode passivated by $SiNx/Al_2O_3$ bilayer. Infrared Physics and Technology. 109, 103389 (2020)

[6] W. D. Hu, Z. H. Ye, L. Liao, H. L. Chen, L. Chen, R. J. Ding, L. He, X. S. Chen, W. Lu.:128 x 128 long-wavelength/mid-wavelength two-color HgCdTe infrared focal plane array detector with ultralow spectral cross talk. Optics Letters. 39(17), 5184-5187 (2014).

[7] D. H. Wu, J. K. Li, A. Dehzangi, M. Razeghi.: High performance InAs/InAsSb Type-II superlattice mid-wavelength infrared photodetectors with double barrier. Infrared Physics and Technology. 109, 103439 (2020)

[8] Y. F. Liu, C. J. Zhang, X. B. Wang, J. Wu, L. Huang.: Interface investigation of InAs/GaSb type II superlattice for long wavelength infrared photodetectors. Infrared Physics and Technology. 113, 103573 (2021)

[9] W. D. Hu, X. S. Chen, Z. H. Ye, W. Lu.: A hybrid surface passivation on HgCdTe long wave infrared detector with in-situ CdTe deposition and high-density Hydrogen plasma modification. Applied Physics Letters. 99(9), 091101 (2011).

[10] L. Q. Zhu, Z. Deng, J. Huang, H. J. Guo, L. Chen, C. Lin, B. L. Chen.: Low frequency noise-dark current correlations in HgCdTe infrared photodetectors. Optics Express. 28(16), 23660-23669 (2020)

[11] L. Wang, Z. H. Chen, J. J. Xu, F. Dong, F. F. Wang, Z. Z. Bai, Y. Zhou, X. L. Chai, H. L, R. J. Ding, J. X. Chen, L. He.: Fabrication and Characterization of InAs/GaSb type-II Superlattice Long-Wavelength Infrared Detectors Aiming High Temperature Sensitivity. IEEE Journal of Lightwave Technology. 38(21), 6129-6134 (2020)

[12] M. Carras, J. L. Reverchon, G. Marre, C. Renard, B. Vinter, X. Marcadet, V. Berger.: Interface band gap engineering in InAsSb photodiodes. Applied Physics Letters. 87(10), 102103 (2005)

[13] Ł. Ciura, A. Kolek, J. Jure´nczyk, K. Czuba, A. Jasik, I. Sankowska, E. Papis-Polakowska, J. Kaniewski.: Noise-Current Correlations in InAs/GaSb Type-II Superlattice Midwavelength Infrared Detectors. IEEE Transactions On Electron Devices. 63(12), 4907-4912 (2016)

[14] C. X. Meng, J. L. Li, L. Yu, X. M. Wang, P. Han, F. Yan, Z. H. Xu, J. X. Chen, X. L. Ji.: Investigation of noise source and its impact on photocurrent performance of long wave infrared InAs/GaSb type II superlattice detectors. Optics Express. 28(10), 14753-14761 (2020)

[15] J. Nguyen, D. Z. Ting, C. J. Hill, A. Soibel, S. A. Keo, S. D. Gunapala.: Dark current analysis of InAs/GaSb superlattices at low temperatures. Infrared Physics and Technology. 52(6), 317-321 (2009)

[16] A. Haddadi, S. Darvish, G. Chen, A. M. Hoang, B. M. Nguyen, et al.: Low frequency noise in 1024x1024 long wavelength infrared focal plane array based on type-II InAs/GaSb superlattice. Quantum Sensing and Nanophotonic Devices IX. 8268, 82680X (2012)
[17] A. Geremew, C. Qian, A. Abelson, S. Rumyantsev, F. Kargar, M. Law, A. A. Balandin.: Low-frequency electronic noise in superlattice and random-packed thin films of colloidal quantum dots. Nanoscale. 11(42), 20171-20178 (2019)
[18] Ł. Ciura, A. Kolek, J. Jure´nczyk, K. Czuba, A. Jasik, I. Sankowska, J. Kaniewski.: 1/f Noise modeling of InAs/GaSb superlattice midwavelength infrared detectors. Optical and Quantum Electronics. 50(1), (2018)